Therapeutic Discovery

Molecular Cancer Therapeutics

MicroRNA Regulation of Oncolytic Adenovirus 6 for Selective Treatment of Castration-Resistant Prostate Cancer

Zhenwei Zhang[1,2,3], Xuemei Zhang[3], Kam Newman[1], and Xinyuan Liu[2,4]

Abstract

Almost all patients with advanced prostate cancer progress to castration-resistant stage with limited treatment options. Oncolytic adenoviruses have been actively pursued as potential agents for cancer treatment. Virtually all clinical trials on oncolytic adenovirus are based on serotype 5. However, viral replication in hepatocytes induces severe liver toxicity and limits its systemic administration for metastatic disease. Moreover, rapid clearance of viral particles injected intravenously further hinders the anticancer efficacy. Adenovirus 6 (Ad6) was previously reported to exhibit less liver toxicity and escape Kupffer cells absorption after systemic administration. To further improve its safety, we generated a novel oncolytic adenovirus Ad6miR, in which four copies of binding sites of a liver-specific microRNA miR122 were incorporated into E1A gene of Ad6. miR122 regulation significantly decreased Ad6 replication in hepatocytes and consequently hepatotoxicity because of the negative regulation of miR122. Cytotoxicity assay using primary or established prostate cancer cell lines showed robust oncolytic activity of Ad6miR. Systemic treatment of established tumors with Ad6miR showed strong antitumor activity, comparable with that of Ad6 or Ad5. Although Ad6 evaded Kupffer cells, its blood clearance rate was as rapid as Ad5. The vast majority of Ad6 particles intravenously injected localized in liver sinusoidal endothelial cells rather than previously reported Kupffer cells. Elevating Ad6miR injection dose increased circulating Ad6miR concentration and its antitumor efficacy. miR122 regulation of Ad6 significantly improves its safety profile after systemic administration, which allows increasing therapeutic doses leading to improved anticancer efficacy of systemic treatment of castration-resistant prostate cancer. *Mol Cancer Ther; 11(11); 2410–8. ©2012 AACR.*

Introduction

For the past 70 years, androgen deprivation achieved by chemical or surgical castration, has been the standard of care for men with prostate cancer. However, the response to treatment is not durable, and with time, the disease often progresses invariably into the fatal castration-resistant prostate cancer (CRPC; 1, 2). Despite some promising preliminary results from new treatments designed to block androgen receptor activity (such as MDV3100 and abiraterone), it is still uncertain that androgen receptor reactivation is the only cause of castration resistance or that abrogation of androgen receptor signaling will result in cure (3).

Virotherapy represents one of the most intensely studied gene therapy strategies for a variety of malignancies, including prostate cancer. It uses genetically engineered viruses for selective infection and killing of tumor cells while sparing normal cells. Several clinical trials using oncolytic adenoviruses have been carried out and promising results have been reported (4–7).

Human adenovirus serotype 5 (Ad5) is the most extensively used platform for the development of oncolytic Ad. However, recently we and other groups found that binding of blood coagulation factors (particularly factor X) to Ad5 hexon mediates the hepatocytes uptake of Ad5, resulting in intolerable hepatotoxicity after i.v. injection for systemic treatment (8–12). Moreover, when Ad5-based oncolytic vectors are intravenously injected for treatment of metastatic disease, much of its full potential has been limited by: (i) rapid removal of virions by the reticuloendothelial system, particularly liver Kupffer cells (KC) as previously reported (13–15); (ii) preexisting neutralizing antibody against Ad5 in up to 90% of human subjects (12, 16, 17).

Authors' Affiliations: [1]Department of Medicine, NorthShore University HealthSystem, University of Chicago, Evanston, Illinois; [2]Institute of Biochemistry and Cell Biology, Shanghai Institutes for Biological Sciences, Chinese Academy of Sciences, Shanghai, China; [3]Department of Nuclear Medicine, Tongji Hospital, Tongji Medical College, Huazhong University of Science and Technology, Wuhan, China; and [4]Xinyuan Institute of Medicine and Biotechnology, College of Life Sciences, Zhejiang Sci-Tech University, Hangzhou, China

Note: Supplementary data for this article are available at Molecular Cancer Therapeutics Online (http://mct.aacrjournals.org/).

Corresponding Authors: Zhenwei Zhang, Department of Medicine, NorthShore University HealthSystem, University of Chicago, 2650 Ridge Avenue, Evanston, IL 60201. Phone: 847-570-1246; Fax: 847-733-0212; E-mail: zhenwei.zhang@hotmail.com, zwzhang@uchicago.edu; and Xinyuan Liu, Institute of Biochemistry and Cell Biology, Shanghai Institutes for Biological Sciences, Chinese Academy of Sciences, 320 Yueyang Rd, Shanghai 200031, China. Phone: 86-21-54921126; Fax: 86-21-54921127; E-mail: xyliu@sibs.ac.cn

doi: 10.1158/1535-7163.MCT-12-0157

The existence of more than 50 human and more than 100 nonhuman Ads with differences in tropism, safety, and seroprevalence suggests the possibility of increasing the portfolio of therapeutic adenoviruses by choosing those with most attractive features (12, 13, 18). Ad6, although belongs to species C as Ad5, was reported to have 40% less of charge clusters in hypervariable regions (HVR) of hexon as compared with Ad5 (13). Replacement of Ad5 HVRs with Ad6 HVRs significantly decreased recognition and absorption by KCs, indicating that Ad6 might be one of the potential candidate adenoviruses (12, 13, 19).

To further detarget hepatocytes after systemic administration of Ad6, we hypothesized that silencing Ad6 E1A gene by a liver-specific microRNA would prevent the viral replication in hepatocytes, although not altering its antitumor effects. MicroRNAs are expressed in tissue-specific and differentiation state-specific patterns and are often differentially expressed or deleted in various cancers (20, 21). Recent studies show that endogenous microRNAs could be exploited to control Ad5 replication. Incorporation of the tissue-specific microRNA target sequences into E1A expression cassette selectively suppressed the Ad5 replication in normal tissues and decreased the virus-related systemic toxicity, although maintained the comparable antitumor efficacy after i.v. injection (22–25). MicroRNA miR122 is one of the candidates, which is abundantly expressed only in hepatocytes (26, 27). Therefore, we incorporated the complementary sequences for miR122 into the E1A expression cassette of Ad6 and generated a novel posttranscriptional liver-detargeted Ad6, designated Ad6miR. Our data show that Ad6miR further reduces the liver toxicity to normal level after systemic delivery; liver sinusoidal endothelial cells (LSEC), rather than generally recognized KCs, might serve as the major scavenger for the rapid clearance of Ad6 from blood circulation. Improved liver safety of Ad6miR allows increasing injection doses, which increases the anticancer activity against CRPC.

Materials and Methods

Adenoviruses and cells

Ad6 was obtained from American Type Culture Collection (ATCC). Ad6 genomic DNA was extracted from infected A549 cells (28); the plasmid containing the Ad6 and Ad6miR genomic DNA were constructed as indicated in Fig. 1. All viruses were generated by transfecting 293 cells and grown in A549 cells. Purified virus stocks were titred with OD260 using standard protocol (8). *dl*309 was used as wide-type Ad5.

All cell lines were purchased from ATCC except where indicated. Human hepatocellular carcinoma cells HepG2 and Huh7, lung cancer A549, HEK293, and murine monocyte-macrophage cells RAW264.7 were cultured in Dulbecco's Modified Eagle's Medium (DMEM) with 10% FBS. The normal human lung fibroblasts and normal human hepatocytes (Nheps; Lonza) were cultured in the medium recommended by the manufacturer. Human prostate cancer cells PC3 and DU145 were maintained in RPMI 1640 medium plus 10% FBS. All cells lines were passaged within 6 months of receiving from the established cell bank and characterized with DNA profiling by the cell bank. The cells were tested to be *Mycoplasma* free by PCR methods before this study. All metastatic bone cancer samples were collected from patients with pathologically confirmed bone metastatic prostate cancer under the written informed consent and protocols approved by the

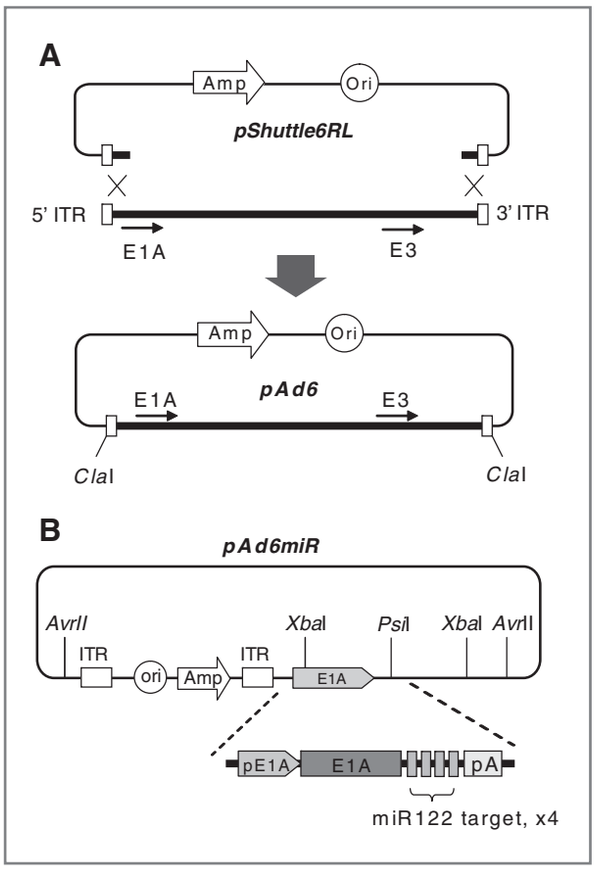

Figure 1. Construction of Ad6- and miR122-regulated Ad6miR. A, construction of Ad6 genomic DNA. A fragment containing the 16 bp of the right and left terminal of Ad6 genomic DNA was synthesized, with a *Sna*BI site at the middle of the terminals and a *Cla*I site flanking each end. The fragment was cloned into *Cla*I-cut pBR322 to make pShuttle6RL. To make the plasmid carrying Ad6 genomic DNA, pAd6, homologous recombination was catalyzed with In-Fusion enzyme between *Sna*BI-cut pShuttle6RL and the linear Ad6 genomic DNA extracted from infected A549 cells, following the manufacturer's instruction (Clontech). B, construction of Ad6miR genomic DNA. A 781-bp fragment containing the sequence between *Xba*I and *Psi*I of Ad6 was synthesized with 4 copies of miR122 target sequence inserted within 3′ untranslated region (UTR) of E1A expression cassette. The smaller fragment of *Xba*I-cut Ad6 genomic DNA containing E1A gene was cloned into pUC19 to make pUC19XbaI. The synthesized fragment restricted with *Xba*I and *Psi*I was cloned into pUC19XbaI with 2-step ligation to make pUC19miR. The smaller fragment of *Avr*II-cut pAd6 was self-ligated to make pBRAvr. The *Xba*I-flanked sequence of pBRAvr was replaced with that of *Xba*I-cut pUC19miR, to make the shuttle vector pBRmiR. The *Avr*II-cut pBRmiR and the larger fragment of *Xba*I-cut pAd6 were cotransformed into BJ5183 to make pAd6miR. Purified viral DNA was transfected into A549 cells to make Ad6miR. ITR, inverted terminal repeat.

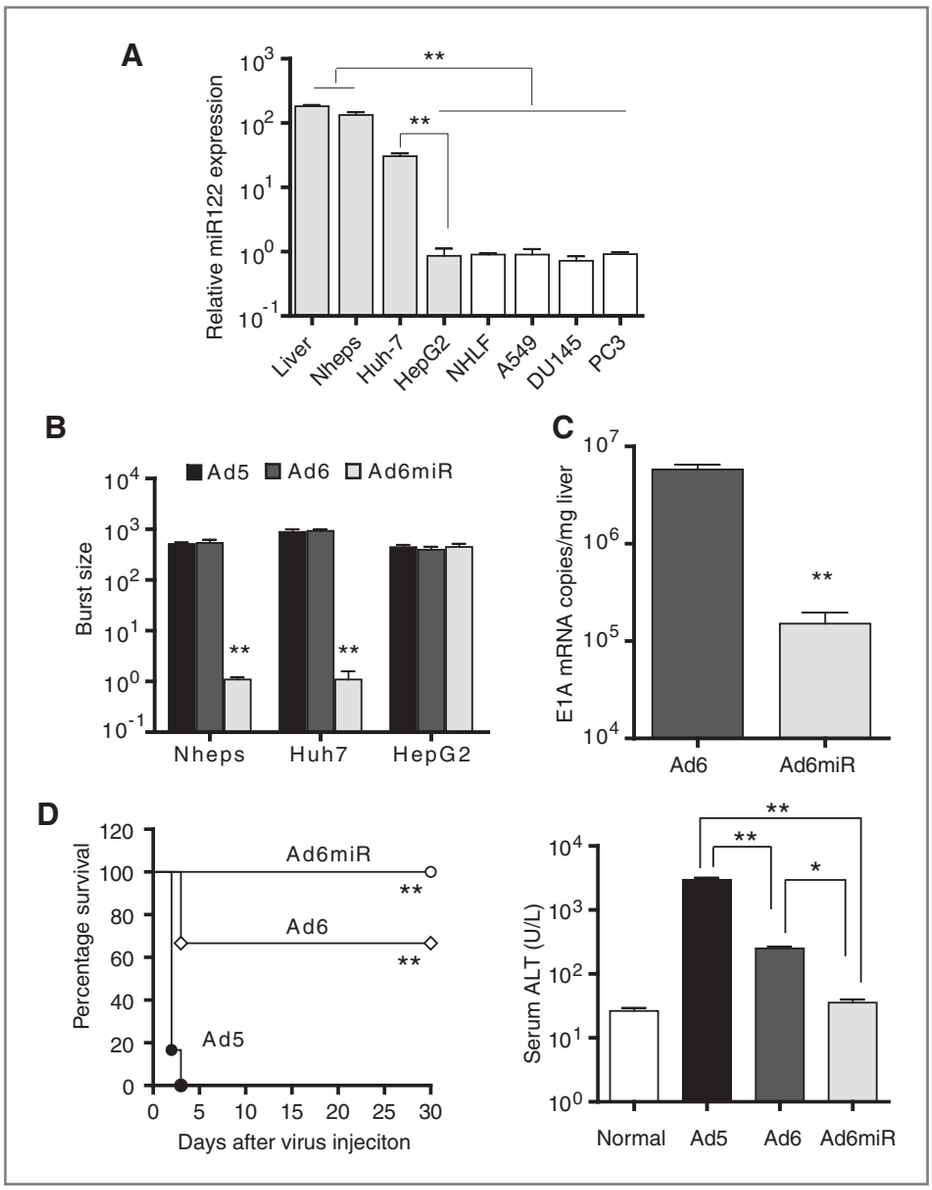

Figure 2. miR122 regulation of viral replication reduces liver toxicity of Ad6miR. A, endogenous miR122 expression in normal and cancer cells. cDNAs were synthesized using 1 μg of total RNA from Balb/c mice liver extraction, normal human hepatocytes, and a panel of cell lines. miR122 levels were quantified using quantitative RT-PCR. Data are normalized with U6 RNA ($n = 3$ for liver samples; $n = 6$ for cell lines). **, $P < 0.01$. B, selective suppression of viral replication *in vitro*. HepG2 and Huh7 cells were infected with Ad6 or Ad6miR at MOI of 100 vp/cell for 2 hours. After 3 times washing, fresh medium was added (day 0). On day 3, cells and supernatants were collected and total infectious virus yield was determined on 293 cells. **, $P < 0.01$. C, miR122-specific silencing of E1A expression *in vivo*. Balb/c mice were injected intravenously with 3×10^{10} vp of Ad6 or Ad6miR ($n = 6$). Seventy-two hours after virus injection, E1A mRNA levels in liver were analyzed. Liver genomic DNA was isolated and viral genomic DNA was determined with qPCR (D). **, $P < 0.01$. D, Kaplan–Meier survival curves (left). BALB/c mice were injected intravenously with 2.0×10^{11} vp per mouse of Ad5, Ad6, or Ad6miR. Moribund mice were sacrificed. Blood was collected and serum ALT levels were analyzed (right). $n = 6$; *, $P < 0.05$; **, $P < 0.01$.

Institutional Review Board. The primary cancer cells were isolated and maintained in DMEM plus Glutamax supplemented with 15% FBS.

Quantification of miR122 and E1A microRNA levels and viral genomic DNA

cDNAs were synthesized using from 1.0 μg extracted total RNA according to standard protocol. Endogenous miR122 expression was then determined with TaqMan MicroRNA Assay Kit (Applied Biosystems). E1A microRNA expression was determined as routine quantitative real-time PCR (RT-PCR). Amplification of mouse or human small nuclear RNA U6 served as an endogenous control to normalize the miRNA expression data. Viral genomic DNA was quantified by qPCR as previously reported (8).

Viral production assay and cell viability assay

Cells were infected with adenoviral vectors [100 viral particles (vp)/cell]. Viral titers of 3 and 48 hours samples were determined as described earlier (8). Viral burst size was calculated by dividing viral titers of 48-hour samples by that of 3-hour samples. For cytotoxicity assay, DU145 and PC3 cells were infected at indicated multiplicity of infection (MOI). Primary prostate cancer cells from patients were infected at MOI of 100 vp/cell. Cell viability was measured on day 5 after infection by MTT assay.

Measurement of serum ALT levels

To determine hepatotoxicity, Balb/c mice were injected intravenously with 2×10^{11} vp per mouse for each Ad and blood was collected 3 days after i.v. injection. Serum

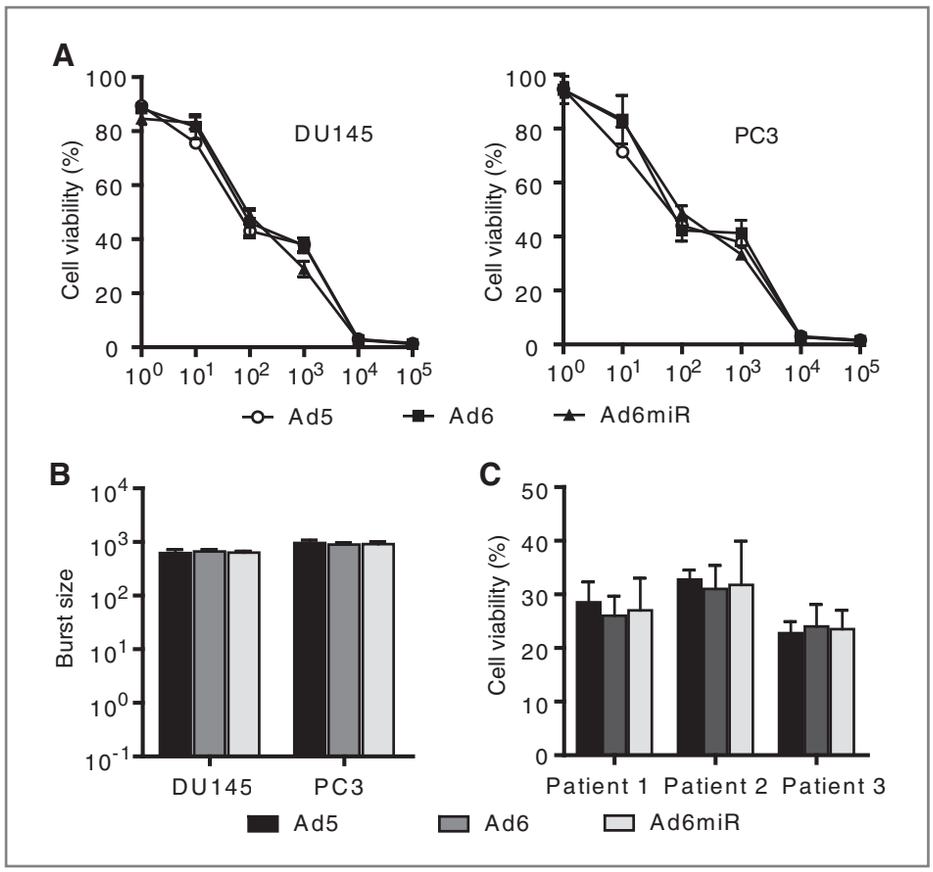

Figure 3. *In vitro* oncolytic activity in prostate cancer cells. A, viral replication in prostate cancer cells. DU145 and PC3 cells were infected and virus yield was determined as described in Fig. 2B. B, prostate cancer cells were infected and cytotoxicity was determined with MTT assay. Cell viability was calculated as a percentage with respect to cells without adenovirus infection. C, primary cancer cells were isolated from pathologically confirmed CRPC patients. Cells were infected at MOI of 100 vp/cell for 5 days and cytotoxicity was determined with MTT assay.

alanine aminotransferase (ALT) levels were measured with an assay kit (JLBio).

Blood clearance and immunofluorescence staining

Balb/c mice received 3×10^{10} vp/mouse via tail vein. Retroorbital sinus blood was collected 1, 5, 10, and 30 minutes after injection. Viral genomes were measured with qPCR assays and plotted as the decay of blood-borne virus versus time. At the zero time point, the concentration was calculated as dose injected divided by mouse weight (29, 30).

To visualize virus distribution in liver, 1 minute after viral injection, the livers were harvested as rapidly as possible and processed for frozen sectioning, followed with immunofluorescence staining. Liver sections were first treated with endogenous biotin blocking reagent (Invitrogen). Following washing with PBS Triton buffer for 30 minutes sections were incubated overnight at 4°C with rabbit anti-mannose receptor antibody (Santa Cruz) and biotin-labeled mouse adenovirus antibody (Millipore) to detect LSEC and adenovirus, respectively. Then the sections were labeled with Alexa Fluor 594 (red)-conjugated goat anti-rabbit antibody and Alex Fluor 488 (green)-conjugated streptoavidin (Invitrogen). Mouse adenovirus antibody was conjugated with biotin labeling kit (Invitrogen). Quantitative analysis was conducted with Image J.

Tumor xenograft in nude mice

All animal experiments were carried out according to the provisions of the Animal Welfare Act and the NIH Guide for the Care and Use of Laboratory Animals. Male nude mice (4–5 weeks of age) were inoculated subcutaneously with 2×10^6 DU145 cells/mouse. When the tumor volume reached from 100 to 170 mm^3, the mice were randomly assigned into 4 groups ($n = 9$). Mice were treated with 2 i.v. injections of 100 μL of buffer or 3×10^{10} vp of Ad5, Ad6, or Ad6miR in 100 μL volume on day 0 and day 3. Measurements of tumor volumes were taken once a week.

To test whether increased dosage of intravenously injected virus could affect the concentration of blood-borne virus, tumor-bearing mice received 1×10^{11} vp/mouse. To evaluate the consequent anticancer efficacy, mice with DU145 s.c. tumors were injected via tail vein with 1×10^{11} vp/mouse of each virus weekly for 3 times. Tumor size were measured and compared with the low dose group (3×10^{10} vp/mouse). In-blood and in-tumor viral genomes were determined with qPCR assays as described above.

Statistical analysis

Statistical analyses were done with Student t test to determine the significance. *In vivo* survival data were analyzed using Kaplan–Meier method with the log-rank

test. $P < 0.05$ was considered statistically significant. *In vitro* experiments were carried out in triplicate or as indicated. All values represent the mean ± SEM.

Results

miR122 regulation in Ad6miR selectively suppresses E1A expression and viral replication in liver

miR122 is an abundant liver-specific microRNA in human liver and rodent liver. RT-PCR analysis showed that miR122 levels were significantly higher in normal human liver cells Nheps and isolated mouse liver cells than HepG2, A549, and prostate cancer cells DU145 and PC3 ($P < 0.01$, vs. Nhep3, Fig. 2A). Notably, Huh7 cells, a relatively well-differentiated hepatocarcinoma cells and always used as hepatocyte model, remained high expression of miR122, as compared with the poorly differentiated HepG2 ($P < 0.01$).

Then we examined whether different miR122 levels would necessarily produce variance of viral replication of Ad6miR. As shown in Fig. 2B, Ad6miR replication was significantly suppressed in normal liver cells Nheps and miR122 positive Huh7 cells ($P < 0.01$, Ad6miR vs. Ad6), whereas comparable viral replication was observed in miR122 negative hepatocarcinoma cells HepG2 ($P > 0.05$, Ad6miR vs. Ad6), suggesting selective suppression of viral replication because of the incorporation of miR122 complementary sites. To test this liver-specific negative control pattern *in vivo*, 3×10^{10} vp of each virus was injected intravenously into Balb/c mice. E1A mRNA was significantly downregulated in Ad6miR group (Fig. 2C, $P < 0.01$).

miR122 regulation of Ad6 E1A further improves liver safety after systemic administration

To evaluate the safety of the posttranscriptional liver-detargeted Ad6miR, we elevated the injection dose to 2×10^{11} vp/mouse. All mice received Ad5 became moribund and were euthanized, which is correlated with the extremely high ALT levels ($P < 0.01$, vs. buffer, Fig. 2D left). Although Ad6 and Ad5 belong to the same species C, Ad6 exhibited less hepatotoxicity ($P < 0.01$, vs. Ad5) and more than 60% of mice survived ($P < 0.01$, vs. Ad5). Conversely, all mice remained healthy in Ad6miR group ($P < 0.01$, vs. Ad5). The survival rate was not statistically different between Ad6 and Ad6miR. However, Ad6 induced higher serum ALT levels than Ad6miR (Fig. 2D right, $P < 0.05$), indicating that systemic administration of Ad6 induced moderate liver damage, although the levels were lower than Ad5 group ($P < 0.01$). In contrast, Ad6miR injection did not increase ALT levels ($P > 0.05$ vs. buffer), suggesting further improved liver safety.

Inhibition of CRPC cell growth *in vitro*

To evaluate whether Ad6miR maintains oncolytic activity, cell viability assay was conducted in DU145 and PC3 cells. As shown in Fig. 3A, there was no significant difference between the oncolytic activity of Ad5 and Ad6 ($P > 0.05$). Interestingly, Ad6miR exhibited comparable cytotoxicity ($P > 0.05$, vs. Ad6). We then assessed the amplification ability of these viruses with infection of 100 vp of each virus. There was no difference between viral replication of Ad5- and Ad6-based viruses in the prostate cancer cells (Fig. 3B, $P > 0.05$), which explained the similar oncolytic capacity. Notably, Ad6miR exhibited similar burst size as compared with Ad6, consistent with the data recently reported on microRNA-regulated Ad5 (23). We also tested the killing efficacy of Ad6miR in primary prostate cancer cells isolated from patients with advanced prostate cancer bone metastasis. After 5 days incubation, Ad6miR killed about 70% of the patient advanced cancer cells, which is comparable with Ad6 and Ad5 (Fig. 3C, $P > 0.05$), suggesting robust cytotoxicity of Ad6miR in patients' CRPC cells.

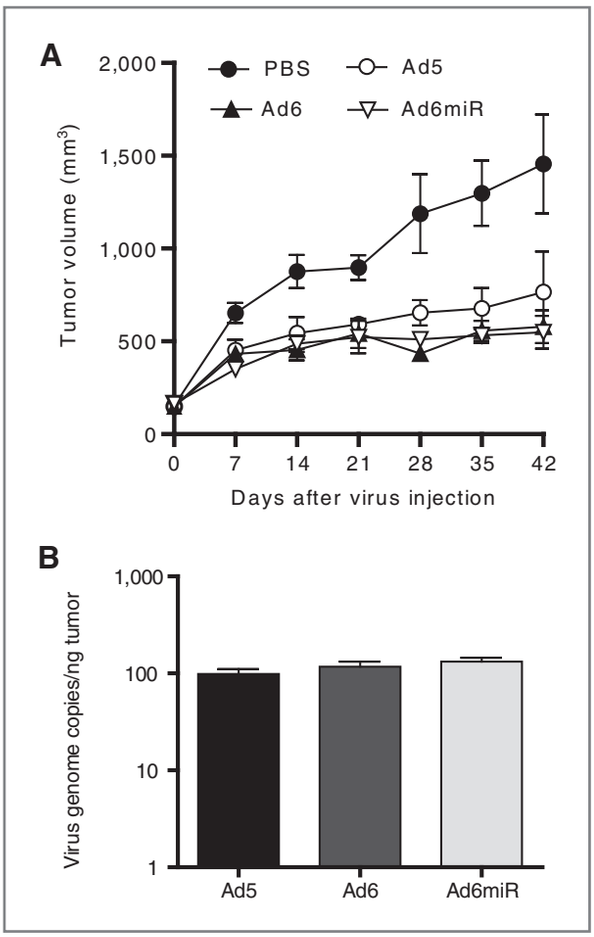

Figure 4. Antitumor activity of Ad6miR in established tumor model. A, mice bearing subcutaneously established DU145 tumors received 2 i.v. injections of 100 μL of buffer or 3×10^{10} vp of Ad5, Ad6, or Ad6miR ($n = 9$) in 100 μL volume on day 0 and day 3. Mice were euthanized when tumor volume reached 2,000 mm^3. B, viral genome copies in tumor. In a separated experiment, tumor-bearing mice were treated with 3×10^{10} vp of each virus. Tumor tissues were collected 24 hours later and viral load were determined with qPCR assays. $n = 6$.

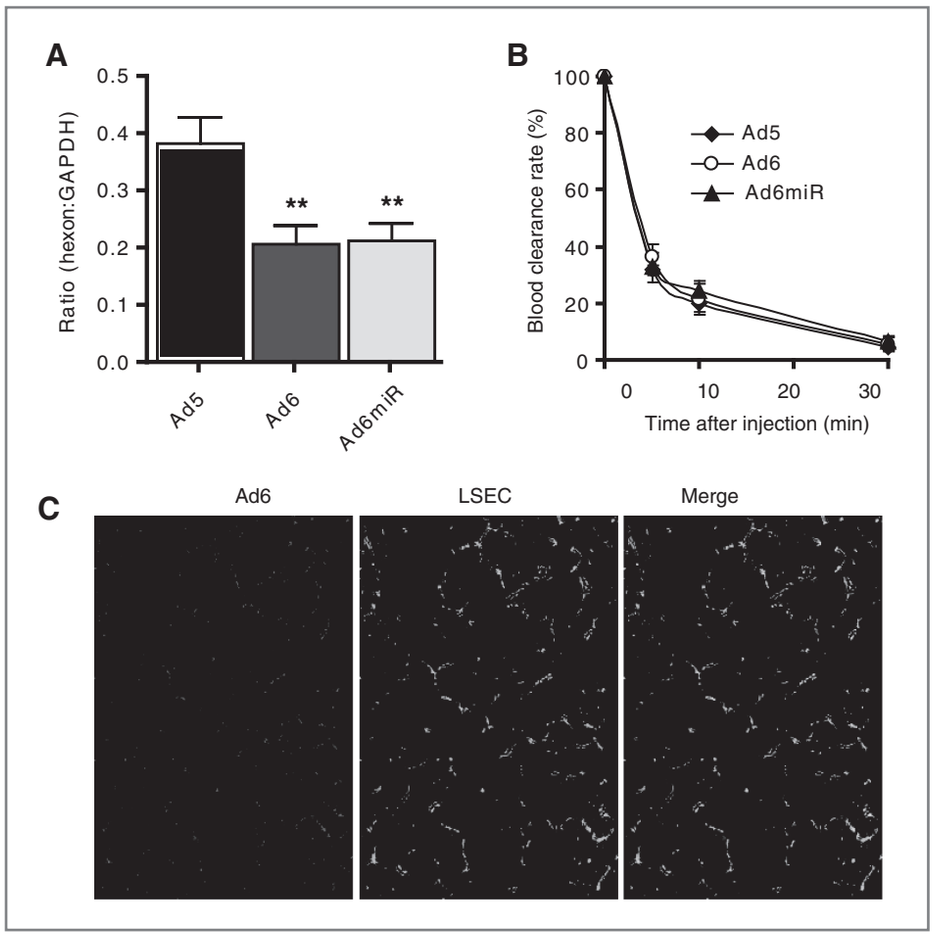

Figure 5. Ad6 evades KCs but not LSECs. A, RAW cells were infected with adenovirus at 10,000 vp/cell. Three hours postinfection at 37°C, cells were harvested and genomic DNA was extracted. Viral and cellular genomes were quatified using qPCR with hexon and glyceraldehyde-3-phosphate dehydrogenase (GAPDH) primers, respectively. Data are normalized to cellular genomes. B, clearance of adenoviruses from blood circulation. Balb/c mice received 3.0×10^{10} vp/mouse via tail vein ($n = 6$). Retroorbital sinus blood was collected at indicated time. Ad genomes were measured with qPCR. **, $P < 0.01$. C, immunofluorencense staining. One minute after viral injection via tail vein, livers were harvested as rapidly as possible. After being processed for frozen sectioning, liver samples were subjected to immunofluorescence staining. The merged images show colocalization of fluorescence. Original magnification, ×100.

Antitumor activity of Ad6miR in prostate cancer model *in vivo*

We treated mice bearing DU145 subcutaneous tumors by 2 i.v. injections of 3×10^{10} vp of Ad5, Ad6, or Ad6miR on day 0 and day 3 via tail vein. Systemic treatment with all viruses produced significant inhibition of tumor growth (Fig. 4A, $P < 0.01$, vs. buffer). Ad6 or Ad6miR produced stronger tumor growth inhibition than Ad5, but the suppressing activity did not reach statistical significance. Considering the liver toxicity of Ad5, we could not compare the dose-dependent antitumor efficacy with elevated doses. In agreement with the *in vitro* cytotoxicity against prostate cancer cells, miR122-regulated viral regulation did not compromise its *in vivo* antitumor effect against CRPC.

Although both Ad6 and Ad5 belong to species C, previous studies have shown that Ad6 interacts differently with KCs when compared with Ad5 (12, 13, 19), which theoretically would improve antitumor effect of Ad6 as compared with its counterpart. On the contrary, data here and elsewhere (12) show that the antitumor effect of KCs evading Ad6 was not more efficacious than Ad5, at least statistically. Therefore, we determined the viral genomes in tumor tissues. Mice with established tumors were intravenously injected 3×10^{10} vp of Ad5 or Ad6. As shown in Fig. 4B, 24 hours after injection there was no difference between Ad5 and Ad6 ($P > 0.05$), indicating similar viral load in tumors.

Ad6 evades KCs, but not LSECs

We then confirmed the KC-evading capability of Ad6 with mouse macrophages cells. Consistent with previously reported (12, 13), we did find that the phagocytosis effect to Ad6 was significantly lower than that to Ad5 ($P < 0.01$, Fig. 5A), indicating reduced phagocytosis by macrophage cells. However, the blood-borne Ad6 particles were cleared at the same rate as Ad5 (Fig. 5B). In as short as 10 minutes, more than 84% of injected viral particles were removed out of blood circulation; there was not difference between Ad5 and Ad6 in the concentration of virus remaining in blood ($P > 0.05$). Two-color immunofluorescence staining revealed that most injected viral particles colocalized in LSECs, with very sparse virus signals outside LSECs (Fig. 5C). Quantitative analysis showed that as much as 90% of Ad6 signals localized in LSECs, providing suggestive evidence that it is indeed LSECs that bound most virus. Our results from the Ad6 virus are consistent with those recently found with Ad5 (30).

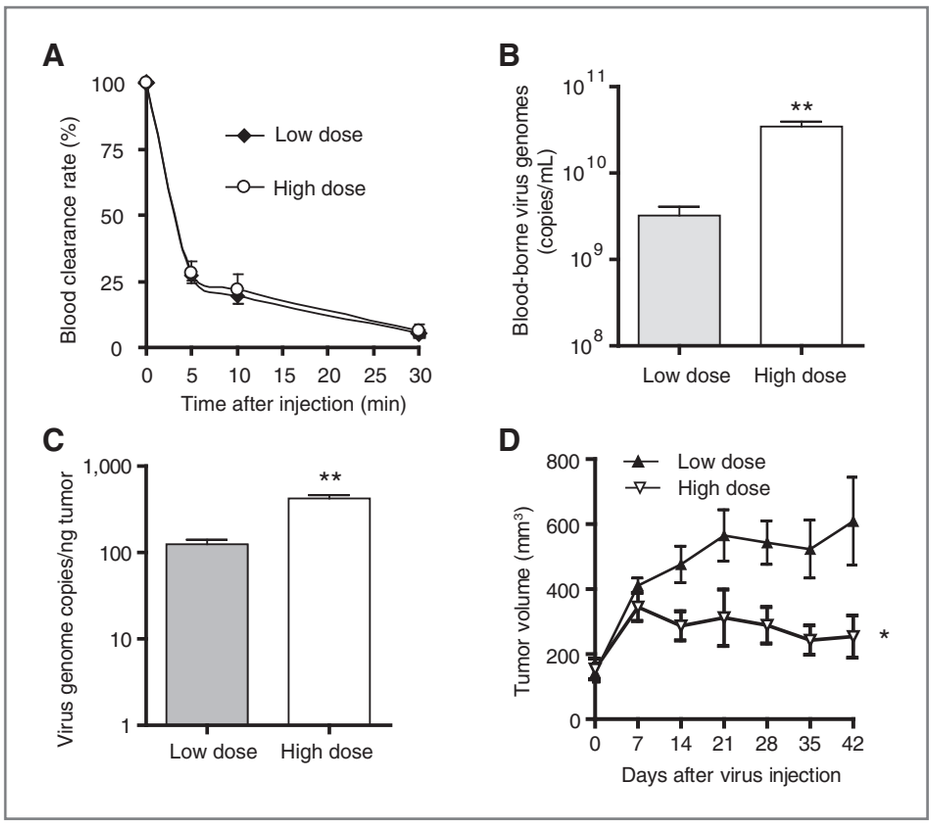

Figure 6. Improved antitumor efficacy with increased injection dosage. A, clearance rate after increasing injection dose. Mice received each virus at 1×10^{11} vp/mouse via tail vein. Blood-borne virus concentration after injection was measured with qPCR assays. Ad genomes were plotted as the decay of blood-borne virus versus time. B, comparison of blood-borne virus concentration at 10 minutes after injection. **, $P < 0.01$. C, viral load in tumor. Tumor-bearing mice were intravenously injected with 1×10^{11} vp/mouse and viral genomes were measured as in Fig. 4B. $n = 3$; **, $P < 0.01$. D, tumor-bearing mice were treated with i.v. injection of 1.0×10^{11} vp/mouse weekly for 3 times. Tumor size was monitored as in Fig. 5A. $n = 9$; *, $P < 0.05$.

Improved anticancer efficacy with increased injection dose

Substantially increased systemic safety of Ad6miR allowed us to examine whether higher injection doses might elevate the concentration of blood-borne virus. When the injection dose was increased to 1×10^{11} vp/mouse, the circulating Ad6miR was removed from blood as rapidly as that of lower dose (Fig. 6A). However, the blood concentration at 10 minutes after virus injection was significantly higher than that in the lower dose; the viral genomes in tumor were also significantly increased (Fig. 6B and C, $P < 0.01$). Correspondingly, the antitumor efficacy was also significantly improved as compared with that of the lower dose group (Fig. 6D, $P < 0.05$).

Discussion

CRPC remains a major clinical challenge, given the complex signal transduction network and readily escaping from single targeting therapy (31), such as androgen deprivation. The potential for Ad5-based virotherapy for CRPC has been hampered by unacceptable systemic toxicity after i.v. injection. In this study, we found that with miR122 regulation in Ad6 the virotherapy-related liver toxicity was virtually reduced to normal level. Moreover, we showed that LSECs might be the dominant virus uptaker in liver and responsible for the rapid removal of blood-borne virus. Taking the advantage of safety profile of Ad6miR, we could increase the i.v. injection dose, which exhibits even more potent antitumor efficacy against CRPC.

miR122 was reported to be a liver-specific microRNA (32). Our data here show abundant expression of miR122 in both normal human hepatocytes and mouse livers, whereas its expression was extremely low in cancer cells including the 2 CRPC cell lines DU145 and PC3 (Fig. 2A). Silencing E1A gene in Ad6miR substantially enhanced liver safety due to the stringent posttranscriptional hepatocyte-detargeting capacity of Ad6miR (Fig. 2D), which is consistent to the published findings in Ad5 (23). In good agreement with the miR122 expression profile of the prostate cancer cell lines, Ad6miR exhibited similar anticancer activity in the CRPC model as compared with Ad6 *in vitro* (Fig. 3) and *in vivo* (Fig. 4A). Difference in viral replication between cancer cells and hepatocytes may well be due to variations in miR122 expression. Of note, in primary cell samples from CRPC patients, Ad6miR exhibited comparable antitumor effect to Ad6 or Ad5 (Fig. 3C), suggesting that Ad6miR maintains the robust antitumor activity.

Until recently, the most widely studied serotype for oncolytic adenovirus is Ad5, which exhibits natural tropism to liver, resulting in rapid clearance from circulation and liver sequestration after systemic administration. The predominant underlying mechanism had been recognized as engulfing and destroying intravenously injected Ad5 by KCs (13, 33). Barry and colleagues reported that

Ad6 possessed KCs-evading capability and replacement of the HVRs of Ad5 with those of Ad6 enabled the hexon-chimaeric virus to evade KCs (13). In agreement with the previous report, we found that Ad6 and Ad6miR were less efficiently phagocytosed by monocyte-macrophage cells (Fig. 5A). However, KC evasion did not translate into slower blood clearance of Ad6 as compared with Ad5 (Fig. 5B), which challenges the scavenging properties of KCs. It has been shown that a very substantial amount of Ad5 was uptake by liver even in KCs depleted mice or when KC uptake has been inactivated (34, 35). Indeed, immunofluorescence staining results suggest that the uptake by LSECs might account for the rapid clearance of KCs-evading Ad6 (Fig. 5C). Recently, Ganesan and colleagues showed with immunofluorenscence staining that the long overlooked LSEC was the major scavenger for rapid and efficient clearance of blood-borne Ad5 (30). Electron microscopy analysis also showed that the fenestrae diameter of LSECs may determine the uptake of circulating adenoviral vectors (34, 36) in mice. In contrast, for larger viral particles such as lentivirus, KCs, instead of LSECs may serve as the main scavenger in liver (37).

So far there are limited choices to reverse the inhibiting effect of LSECs sequestration for virotherapy. Our results suggest that higher injection dose could increase the circulating virus concentration and consequently the viral load in tumor, leading to the more potent anticancer efficacy (Fig. 6B, C, and D). Notably, with the elevated injection dose, the clearance rate from blood remained as rapidly as the lower dose (Fig. 6A), indicating LSECs does reserve a strong "buffering effect" for sequestering blood-borne viruses. Previous reports showed that i.v. injection of low-dose cyclophosphamide exhibits selective disrupt LSECs, although not affecting KCs and hepatocytes (37). Our very preliminary data from nude mice show that cyclophosphamide injection enhanced antitumor effect of Ad6miR (Supplementary Figs. S1 and S2). Unfortunately, because of the residual but unignorable components of immune system in nude mice, the concurrent contribution of immunosuppressing effect of CPA could not be excluded.

Because i.v. injection of Ad6 caused less liver toxicity as compared with that of Ad5 (Fig. 2D), HVRs and/or fiber variance might affect binding of virus to hepatocytes after gaining access through LSECs, although we could not exclude the possibility that the variances might also affect the pinocytosis or transcytosis of LSECs. Other factors (e.g., immunity neutralization) may also involve the fate of LSECs-absorbed virus. Obviously, these questions have to be pursued in further studies using more sophisticated animal models.

Taken together, we generated a novel adenovirus based on Ad6. Significantly improved liver safety allows increasing therapeutic doses of oncolytic adenovirus, leading to increased systemic anticancer efficacy against CRPC.

Disclosure of Potential Conflicts of Interest

No potential conflicts of interest were disclosed.

Authors' Contributions

Conception and design: Z. Zhang, X. Liu
Development of methodology: Z. Zhang, K. Newman, X. Liu
Acquisition of data (provided animals, acquired and managed patients, provided facilities, etc.): Z. Zhang, X. Zhang, K. Newman, X. Liu
Analysis and interpretation of data (e.g., statistical analysis, biostatistics, computational analysis): Z. Zhang, X. Zhang
Writing, review, and/or revision of the manuscript: Z. Zhang, X. Zhang, K. Newman
Administrative, technical, or material support (i.e., reporting or organizing data, constructing databases): Z. Zhang, X. Liu
Study supervision: Z. Zhang, X. Liu

Grant Support

This work was supported by grants from Hi-Tech Research Development Program (863 Program, no. 2007AA021006) and the 973 Project (no. 2004CB518804) from National Nature Science Foundation of China (X. Liu).

The costs of publication of this article were defrayed in part by the payment of page charges. This article must therefore be hereby marked *advertisement* in accordance with 18 U.S.C. Section 1734 solely to indicate this fact.

Received February 15, 2012; revised August 7, 2012; accepted August 9, 2012; published OnlineFirst August 22, 2012.

References

1. de Bono JS, Logothetis CJ, Molina A, Fizazi K, North S, Chu L, et al. Abiraterone and increased survival in metastatic prostate cancer. N Engl J Med 2011;364:1995–2005.
2. Lamoureux F, Thomas C, Yin MJ, Kuruma H, Fazli L, Gleave ME, et al. A novel HSP90 inhibitor delays castrate-resistant prostate cancer without altering serum PSA levels and inhibits osteoclastogenesis. Clin Cancer Res 2011;17:2301–13.
3. Tanaka H, Kono E, Tran CP, Miyazaki H, Yamashiro J, Shimomura T, et al. Monoclonal antibody targeting of N-cadherin inhibits prostate cancer growth, metastasis and castration resistance. Nat Med 2010;16:1414–20.
4. Small EJ, Carducci MA, Burke JM, Rodriguez R, Fong L, van Ummersen L, et al. A phase I trial of intravenous CG7870, a replication-selective, prostate-specific antigen-targeted oncolytic adenovirus, for the treatment of hormone-refractory, metastatic prostate cancer. Mol Ther 2006;14:107–17.
5. Freytag SO, Movsas B, Aref I, Stricker H, Peabody J, Pegg J, et al. Phase I trial of replication-competent adenovirus-mediated suicide gene therapy combined with IMRT for prostate cancer. Mol Ther 2007;15:1016–23.
6. Li JL, Liu HL, Zhang XR, Xu JP, Hu WK, Liang M, et al. A phase I trial of intratumoral administration of recombinant oncolytic adenovirus overexpressing HSP70 in advanced solid tumor patients. Gene Ther 2009;16:376–82.
7. Kimball KJ, Preuss MA, Barnes MN, Wang M, Siegal GP, Wan W, et al. A phase I study of a tropism-modified conditionally replicative adenovirus for recurrent malignant gynecologic diseases. Clin Cancer Res 2010;16:5277–87.
8. Zhang Z, Krimmel J, Hu Z, Seth P. Systemic delivery of a novel liver-detargeted oncolytic adenovirus causes reduced liver toxicity but maintains the antitumor response in a breast cancer bone metastasis model. Hum Gene Ther 2011;22:1137–42.
9. Alba R, Bradshaw AC, Coughlan L, Denby L, McDonald RA, Waddington SN, et al. Biodistribution and retargeting of FX-binding ablated adenovirus serotype 5 vectors. Blood 2010;116:2656–64.

10. Waddington SN, McVey JH, Bhella D, Parker AL, Barker K, Atoda H, et al. Adenovirus serotype 5 hexon mediates liver gene transfer. Cell 2008;132:397–409.
11. Prill JM, Espenlaub S, Samen U, Engler T, Schmidt E, Vetrini F, et al. Modifications of adenovirus hexon allow for either hepatocyte detargeting or targeting with potential evasion from Kupffer cells. Mol Ther 2011;19:83–92.
12. Shashkova EV, May SM, Barry MA. Characterization of human adenovirus serotypes 5, 6, 11, and 35 as anticancer agents. Virology 2009;394:311–20.
13. Khare R, May SM, Vetrini F, Weaver EA, Palmer D, Rosewell A, et al. Generation of a Kupffer Cell-evading adenovirus for systemic and liver-directed gene transfer. Mol Ther 2011;19:1254–62.
14. Xu Z, Tian J, Smith JS, Byrnes AP. Clearance of adenovirus by Kupffer cells is mediated by scavenger receptors, natural antibodies, and complement. J Virol 2008;82:11705–13.
15. Tao N, Gao GP, Parr M, Johnston J, Baradet T, Wilson JM, et al. Sequestration of adenoviral vector by Kupffer cells leads to a nonlinear dose response of transduction in liver. Mol Ther 2001;3:28–35.
16. Roberts DM, Nanda A, Havenga MJ, Abbink P, Lynch DM, Ewald BA, et al. Hexon-chimaeric adenovirus serotype 5 vectors circumvent pre-existing anti-vector immunity. Nature 2006;441:239–43.
17. Nkolola JP, Peng H, Settembre EC, Freeman M, Grandpre LE, Devoy C, et al. Breadth of neutralizing antibodies elicited by stable, homogeneous clade A and clade C HIV-1 gp140 envelope trimers in guinea pigs. J Virol 2010;84:3270–9.
18. Aoki K, Benko M, Davison AJ, Echavarria M, Erdman DD, Harrach B, et al. Toward an integrated human adenovirus designation system that utilizes molecular and serological data and serves both clinical and fundamental virology. J Virol 2011;85:5703–4.
19. Khare R, Chen CY, Weaver EA, Barry MA. Advances and future challenges in adenoviral vector pharmacology and targeting. Curr Gene Ther 2011;11:241–58.
20. Calin GA, Croce CM. MicroRNA signatures in human cancers. Nat Rev Cancer 2006;6:857–66.
21. Volinia S, Calin GA, Liu CG, Ambs S, Cimmino A, Petrocca F, et al. A microRNA expression signature of human solid tumors defines cancer gene targets. Proc Natl Acad Sci U S A 2006;103:2257–61.
22. Ylosmaki E, Hakkarainen T, Hemminki A, Visakorpi T, Andino R, Saksela K. Generation of a conditionally replicating adenovirus based on targeted destruction of E1A mRNA by a cell type-specific MicroRNA. J Virol 2008;82:11009–15.
23. Sugio K, Sakurai F, Katayama K, Tashiro K, Matsui H, Kawabata K, et al. Enhanced safety profiles of the telomerase-specific replication-competent adenovirus by incorporation of normal cell-specific microRNA-targeted sequences. Clin Cancer Res 2011;17:2807–18.
24. Cawood R, Wong SL, Di Y, Baban DF, Seymour LW. MicroRNA controlled adenovirus mediates anti-cancer efficacy without affecting endogenous microRNA activity. PLoS One 2011;6:e16152.
25. Cawood R, Chen HH, Carroll F, Bazan-Peregrino M, van Rooijen N, Seymour LW. Use of tissue-specific microRNA to control pathology of wild-type adenovirus without attenuation of its ability to kill cancer cells. PLoS Pathog 2009;5:e1000440.
26. Lagos-Quintana M, Rauhut R, Yalcin A, Meyer J, Lendeckel W, Tuschl T. Identification of tissue-specific microRNAs from mouse. Curr Biol 2002;12:735–9.
27. Schickel R, Boyerinas B, Park SM, Peter ME. MicroRNAs: key players in the immune system, differentiation, tumorigenesis and cell death. Oncogene 2008;27:5959–74.
28. Hirt B. Selective extraction of polyoma DNA from infected mouse cell cultures. J Mol Biol 1967;26:365–9.
29. Vacha J. Blood volume in inbred strain BALB/c, CBA/J and C57BL/10 mice determined by means of 59Fe-labelled red cells and 59Fe bound to transferrin. Physiol Bohemoslov 1975;24:413–9.
30. Ganesan LP, Mohanty S, Kim J, Clark KR, Robinson JM, Anderson CL. Rapid and efficient clearance of blood-borne virus by liver sinusoidal endothelium. PLoS Pathog 2011;7:e1002281.
31. Alberts B. The challenge of cancer. Science 2011;331:1491.
32. Kutay H, Bai S, Datta J, Motiwala T, Pogribny I, Frankel W, et al. Downregulation of miR-122 in the rodent and human hepatocellular carcinomas. J Cell Biochem 2006;99:671–8.
33. Bilzer M, Roggel F, Gerbes AL. Role of Kupffer cells in host defense and liver disease. Liver Int 2006;26:1175–86.
34. Di Paolo NC, van Rooijen N, Shayakhmetov DM. Redundant and synergistic mechanisms control the sequestration of blood-born adenovirus in the liver. Mol Ther 2009;17:675–84.
35. Manickan E, Smith JS, Tian J, Eggerman TL, Lozier JN, Muller J, et al. Rapid Kupffer cell death after intravenous injection of adenovirus vectors. Mol Ther 2006;13:108–17.
36. Jacobs F, Wisse E, De Geest B. The role of liver sinusoidal cells in hepatocyte-directed gene transfer. Am J Pathol 2010;176:14–21.
37. van Til NP, Markusic DM, van der Rijt R, Kunne C, Hiralall JK, Vreeling H, et al. Kupffer cells and not liver sinusoidal endothelial cells prevent lentiviral transduction of hepatocytes. Mol Ther 2005;11:26–34.